

**Limit on Excitation and Stabilization of Atoms in Intense Optical Laser Fields**H. Zimmermann,<sup>1,\*</sup> S. Meise,<sup>1</sup> A. Khujakulov,<sup>2</sup> A. Magaña,<sup>2</sup> A. Saenz,<sup>2,†</sup> and U. Eichmann<sup>1,‡</sup><sup>1</sup>*Max-Born-Institute, Max-Born-Strasse 2a, 12489 Berlin, Germany*<sup>2</sup>*AG Moderne Optik, Institut für Physik, Humboldt-Universität zu Berlin, 12489 Berlin, Germany*

(Received 9 October 2017; published 22 March 2018)

Atomic excitation in strong optical laser fields has been found to take place even at intensities exceeding saturation. The concomitant acceleration of the atom in the focused laser field has been considered a strong link to, if not proof of, the existence of the so-called Kramers-Henneberger (KH) atom, a bound atomic system in an intense laser field. Recent findings have moved the importance of the KH atom from being purely of theoretical interest toward real world applications; for instance, in the context of laser filamentation. Considering this increasing importance, we explore the limits of strong-field excitation in optical fields, which are basically imposed by ionization through the spatial field envelope and the field propagation.

DOI: [10.1103/PhysRevLett.120.123202](https://doi.org/10.1103/PhysRevLett.120.123202)

Stabilization of atoms in ultrastrong laser fields is an intriguing feature of laser-matter interaction and has been intensively discussed ever since its first initial theoretical trigger [1–3]. The hypothetical existence of bound states of a strongly oscillating electron in a high-frequency electric (laser) field in the vicinity of an ionic core finds its origin in the Kramers-Henneberger (KH) approach [4] and has been shown theoretically [1,5,6], but only isolated experimental demonstrations of stabilization have been achieved so far [7,8].

Recently, several groups have elaborated on the idea that the Kramers-Henneberger approach can be fruitfully applied to low-frequency laser fields [9–11] as well. Atomic stabilization and effects due to the quantum mechanical level structure arising from the KH potential are theoretically shown to be observable even at relatively low laser intensities [12]. The aforementioned investigations were partially fueled by a recent experiment [13] confirming the fact that neutral atoms survive strong near-infrared (NIR) laser pulses. Most noticeable is the concomitant acceleration of the surviving atom in the strong focused inhomogeneous laser field, which leads to a measurable deflection as a result of the strongly oscillating electron. It can be viewed as a strong indication of the existence of KH states [12]. As a far-reaching consequence, KH states have been speculated to strongly influence atomic and plasma dynamics, e.g., via a high-order term of the Kerr effect, which, in turn, is largely responsible for the formation of laser filaments [14,15]. In contrast to the high-frequency case well described in the dipole approximation, low-frequency fields might hamper the formation of KH states by beyond dipole contributions.

In this Letter we explore the limits of atomic excitation and stabilization in strong NIR laser fields imposed by the spatial field envelope and the field propagation. It is known

from earlier experimental investigations and from theoretical studies within the validity of the dipole approximation both classically and quantum mechanically that the excitation of atoms is possible even for laser intensities reaching beyond the saturation intensity [16]. However, it is expected that field gradients as those present in a focused laser beam and the relativistic  $\mathbf{v} \times \mathbf{B}$  drift become important for low-frequency laser fields and essentially hinder the occurrence of bound states, even in the high-frequency regime [17,18]. First experimental indications of the impact of the field gradients in optical fields have been reported [19,20]. Moreover, our investigation extends recent work on studying the influence of nondipole interactions and the Coulomb potential on the electron dynamics [21–23] by looking into the dynamics of the center of mass (c.m.) motion.

We tackle the problem by using an experimental setup which allows for the direct detection of excited atoms after strong-field excitation and simultaneously monitor the atomic deflection in the strong laser field as a sensitive probe to gradient fields inside the laser focus [13]. Using He, with its high ionization potentials for the two electrons, as a target atom, the application of high laser intensities up to  $10 \text{ PW cm}^{-2}$  to study neutral excitation is possible before substantial suppression of the excited-state formation sets in due to ionization of the otherwise uninvolved second electron. We apply semiclassical models [13,24] to identify physical mechanisms responsible for strongly reduced excitation and to finally reach a quantitative understanding. Quantum mechanical single-active-electron time-dependent Schrödinger equation (TDSE) calculations are shown to confirm the classical results.

The experimental setup and the measuring technique have been described elsewhere [13,25]. In brief, a collimated thermal beam of He atoms which is directed toward a

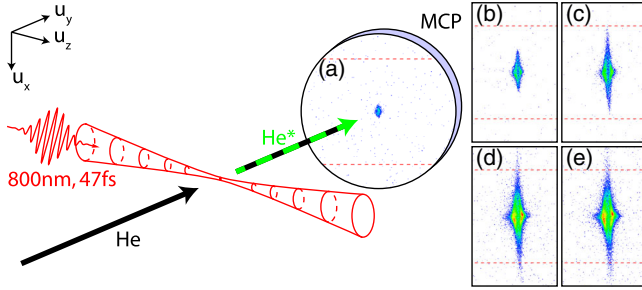


FIG. 1. Schematic sketch of the experimental setup and actual measurements of the atomic distribution on the detector. The laser intensities for (a)–(e) are the same as in Figs. 2(a)–2(e), respectively.

position sensitive multichannel-plate (MCP) detector is intersected by a strong pulsed laser beam focused down to a beam waist  $w_0 = (11.4 \pm 0.2) \mu\text{m}$  which mostly ionizes atoms but also excites a small fraction of them. These atoms are detected if they are still in an excited state when they hit the detector. This is the case since the atoms partially decay into a metastable state which lives long enough [26]. A scheme of the apparatus with actual measurements is shown in Fig. 1.

The experimental data displayed in Fig. 2 show the deflection of atoms which were initially located in the focal plane ( $z = 0 \pm 100 \mu\text{m}$ ). The data are extracted from the full measurements shown in Fig. 1. We can clearly follow the increasing deflection of atoms with increasing laser peak intensity up to  $I_0 = 10 \text{ PW cm}^{-2}$  [Figs. 2(a)–2(c)]. A further increase of the laser intensity substantially diminishes the number of surviving atoms that experience the enhanced deflection [Figs. 2(d) and 2(e)]. Note that, at all

intensities, we do not observe deflection in propagation direction of the laser field.

In order to describe the experimental results theoretically, we exploit the semiclassical model of frustrated tunneling ionization (FTI) [13,24,25] to perform classical-trajectory Monte Carlo calculations. We solve the coupled classical Newton equations for a  $\text{He}^+$  ion and the electron (the subscript values  $i = 1$  and 2, respectively) subjected to the Lorentz force and the Coulomb force  $\mathbf{F}_C$ , with  $q_i$  being the charge and  $\mathbf{v}_i$  the velocity of the electron and the ion, respectively:

$$\mathbf{F}_i = q_i \mathbf{E}_i + q_i \mathbf{v}_i \times \mathbf{B}_i + \mathbf{F}_C. \quad (1)$$

For the electric and magnetic fields  $\mathbf{E}$  and  $\mathbf{B}$ , we use in the first-order approximation the description of a focused Gaussian beam which propagates in the  $u_z$  direction [27] and is linearly polarized in the  $u_x$  direction; see Fig. 1. The initial conditions are given by the tunneling model [25,28,29]. Excited bound states are characterized by negative total energy in the relative motion of ion and electron [24,25]. Additionally, we obtain the momentum transfer to the c.m. of the system which leads to its deflection.

As detailed in the Supplemental Material [30], we identify the two most influential terms emerging from the inclusion of the field envelope,  $E_0 f(t) \exp(-u^2/w_0^2) \times \cos(\omega t - k u_z) \hat{\mathbf{u}}_x + 2(E_0/\omega) f(t) \exp(-u^2/w_0^2) v_{u_x} (u_y/w_0^2) \times \sin(\omega t - k u_z) \hat{\mathbf{u}}_y$  and the field propagation  $(E_0/c) f(t) \exp(-u^2/w_0^2) v_{u_x} \cos(\omega t - k u_z) \hat{\mathbf{u}}_z$ . Here,  $\omega$  is the photon energy,  $k = \omega/c$  is the wave number,  $c$  is the speed of light,  $E_0$  is the electric field amplitude in the  $u_x$  direction and  $f(t)$  is the temporal field envelope,  $u = \sqrt{u_x^2 + u_y^2}$  is the radial

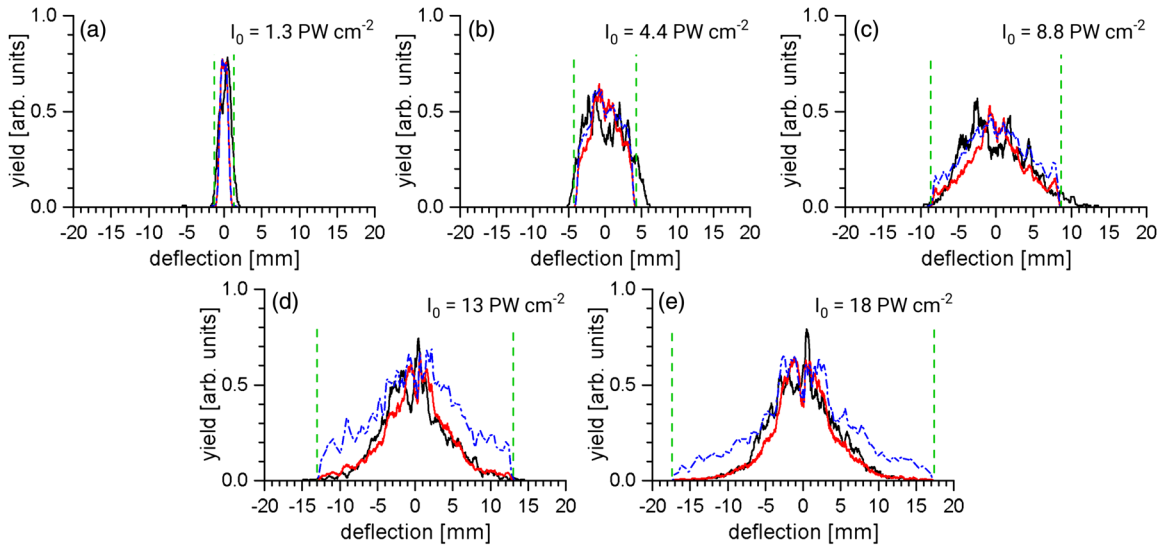


FIG. 2. Measured and calculated deflection of the c.m. of excited atoms after exposing ground state He atoms to laser pulses with the indicated peak intensities  $I_0$  of (a) 1.3, (b) 4.4, (c) 8.8, (d) 13 and (e) 18  $\text{PW cm}^{-2}$ . Experimental data, black curves; calculated distribution for bound trajectories, red (grey) curves; c.m. deflections for unbound trajectories, dashed blue curves. The vertical dashed green lines indicate the limits of deflection.

position in the beam, and  $v_{u_j}$  represents the velocity components of the charged particle. Since the terms are proportional to the laser driven excursion and velocity of the charged particle, they are appreciable only for the light electron and are negligible for the heavy ion. Thus, loosely speaking, they act not only on the relative coordinate but, importantly, also on the c.m. In essence, the first term can be reformulated to recover the ponderomotive or gradient force, which results in momentum transfer to the c.m. The second term, which is associated with the Lorentz drift force, displaces the c.m. negligibly during the laser pulse but does not transfer lasting momentum after the laser pulse has been turned off. However, it influences the final  $n$  distribution since it substantially displaces the electron during the laser pulse. The same is true for the ponderomotive force that acts as a quasiunidirectional static electric field that follows in strength the field gradient, which in turn rises and falls in time with the field envelope. Finally, we note that, at high laser intensities, saturation sets in very early in the laser pulse, prompting the start of the trajectories at the beginning of the pulse. Thus, the electrons gain only limited drift energy, independent of the maximum pulse intensity, which helps them finally to relax into a bound state.

The calculated neutral excited atom yields as a function of the deflection are displayed in Fig. 2. To make a comparison with the experiment, we restrict our analysis to the focal plane. The focal-volume averaging effect along the transversal (radial) direction is intrinsically considered in our calculations. Except for an overall scaling factor, there is no additional fitting parameter involved. The yield of excited atoms is nicely confirmed by the semiclassical calculations. It is also clearly visible in Figs. 2(d)–2(e) that only very few atoms experience the maximum deflection given by the ponderomotive force acting on the c.m. [13]. Obviously, a large portion of the excitation yield is lost due to enhanced ionization. To appreciate the decreasing number of atoms surviving higher deflection, we show for comparison the deflection of the c.m. for those trajectories where the electron does not stay bound. In this case the deflection curve is not subjected to a suppression at the higher intensities and the maximum deflection of the c.m. increases proportional to the intensity gradient at  $w_0/2$ . Given the very good agreement with the experimental data, we are encouraged to analyze in more detail the processes that lead to the suppression of excitation with increasing intensity of the laser pulses.

In Fig. 3 we show the results of a comprehensive analysis of the excited atom yield calculated as a function of the radial distance from the center of the laser field for four different peak intensities. The effective intensity decreases in the focal plane according to  $I(u) = I_0 \exp(-2u^2/w_0^2)$ . The radial intensity gradient  $\nabla I = -4I_0(u/w_0^2) \exp(-2u^2/w_0^2)$  changes nonmonotonically, with a maximum at  $w_0/2$ . The curves are obtained

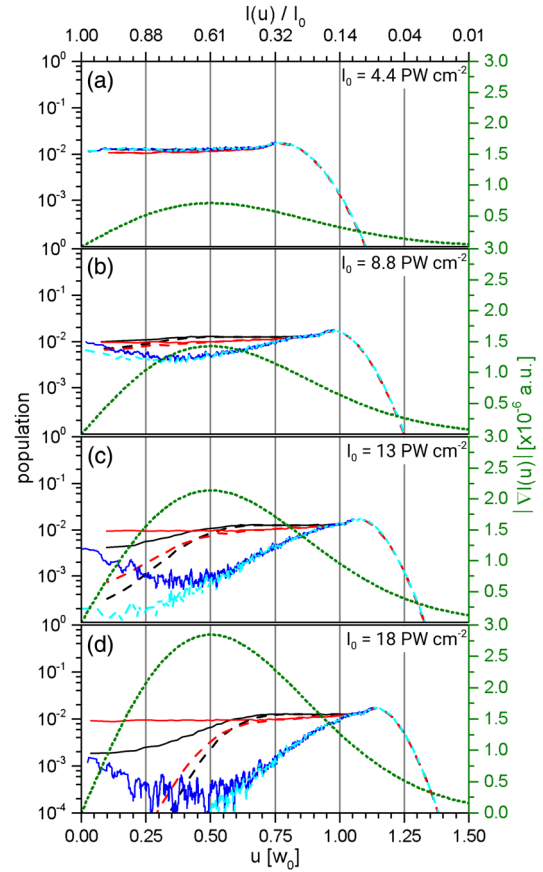


FIG. 3. Population of excited states as a function of the radial distance  $u$  for different peak intensities  $I_0$  of (a) 4.4, (b) 8.8, (c) 13 and (d) 18  $\text{PW cm}^{-2}$ . The upper axis shows the intensity  $I(u)$  normalized to the peak intensity  $I_0$ . The laser field is taken into account in the dipole approximation [the red (grey) curves], a plane-wave approximation (the black curves), and as a full field [the blue (noisy) curves]. The dashed curves give the population with double ionization included, the solid curves without. The dotted green curve gives the intensity gradient with the scale on the right side. Note that the population in the full field calculations [the blue (noisy) curves] oscillate erratically due to the combination of a reduced number of trajectories captured into bound states at high intensity gradients and a lower sampling volume.

by calculating the number of bound trajectories out of a fixed number of initially launched trajectories (typically  $10^4$  per spatial point) and weighting the outcome of the calculations with the overall tunneling probability. The laser field is taken into account in the dipole approximation, as a propagating plane wave, and as a full focused electromagnetic field. Additionally, we have the option to exclude double ionization.

In Fig. 3(a), where we display the results for a peak intensity of  $I_0 = 4.4 \text{ PW cm}^{-2}$ , we find for all three representations of the laser field that the curves are essentially superposable. This indicates the validity of the dipole picture for excitation. Double ionization does not play a role at this intensity. At higher intensities,

Figs. 3(b)–3(d), we first recognize two important features for the dipole versus the plane-wave approximation. While the yields calculated within the dipole approximation stay basically flat toward the peak intensity, the results for the plane-wave field fall substantially below the pure dipole results indicating a strong onset of a reduced FTI process due to field propagation effects. In remarkable contrast, one observes the opposite behavior in the lower intensity regime. Here, the field propagation term actually slightly increases the fraction of bound trajectories. This behavior has also been theoretically observed in high-frequency field stabilization [34]. In our case this fact might become clear when considering that the electron, which is heavily oscillating in the laser field, is pushed away from the ionic core, thus reducing fatal encounters during the laser pulse, while, concomitantly, the drift force does not introduce additional drift momentum. Looking at the ionization weighted yields, one realizes the influence of the double ionization probability, which reduces the yield substantially above an effective intensity  $I > 10 \text{ PW cm}^{-2}$  and results in the steep descents of the curves.

Turning to the full field calculation, Figs. 3(b)–3(d), it is obvious that the curves show a substantial decrease in the formation of bound states around  $w_0/2$ , i.e., around the maximum gradient, which can be attributed mostly to the gradient (ponderomotive) force acting on the system. It is important to note that the decrease in the yield due to the gradient force clearly occurs before double ionization sets in at a high intensity. In any case the spatial field envelope seems to be largely responsible for the strongly reduced excitation in strong optical laser pulses.

The calculations also allow for a conclusive insight on the ramifications that the spatial field envelope and the field propagation have on the Rydberg state distribution. In Fig. 4(a) we show the influence of propagation effects on the  $n$  distribution by approximating the laser field by a plane wave neglecting the spatial field envelope. Only

toward higher peak intensities does the distribution originally centered around  $n = 10$  drop, which indicates a strong reduction of excited states. Simultaneously, a second maximum evolves which shifts toward larger  $n$  values with increasing intensity. In Fig. 4(b) we show the influence of the spatial field envelope on the  $n$  distribution at a comparably low peak intensity of  $5.3 \text{ PW cm}^{-2}$ . By increasing the gradient, i.e., effectively focusing more tightly but keeping the peak intensity fixed, the population in the center of the distribution drops without exhibiting a second maximum nor affecting higher  $n$  states. In Fig. 4(c) we compare the results for various approximations of the laser field. Obviously, the main decrease in the  $n$  distribution comes from the spatial field envelope and is only minorly influenced by the field propagation. At a higher peak intensity, the effect of both terms becomes similar, exhibiting a shift in the  $n$  distribution—but only on a very low level.

Finally, the classical calculations including the spatial field envelope are essentially backed by quantum mechanical calculations; see Fig. 4(e) and the detailed information in the Supplemental Material [30]. Here, at a peak intensity of  $10 \text{ PW cm}^{-2}$  states around  $n = 10$  are diminished in comparison with calculations that do not include spatial field effects. Although the spatial field effects formally resemble a Stark Hamiltonian, where one could expect ionization to occur from high  $n$  to low  $n$  values, the outcome leaves the formation of high Rydberg states unaffected and ionizes, basically, states around  $n = 10$ .

In conclusion, we have studied experimentally the limits on atomic excitation in strong laser fields. Using an experimental technique that allows for a direct measurement of excited states by simultaneously recording the c.m. motion of the surviving atom, we are able to analyze the excitation yield within the focal plane. Comparing our results to a semiclassical calculation, we find, for 45 fs long pulses, that at laser intensities above  $10 \text{ PW cm}^{-2}$  spatial

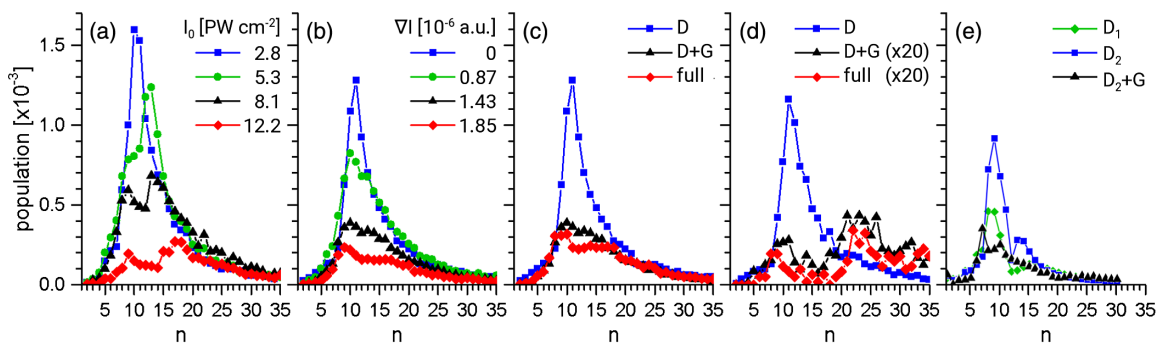


FIG. 4. The  $n$  distributions (a) for a plane wave at different peak intensities, (b) for dipole approximation at a fixed effective intensity of  $I = 5.3 \text{ PW cm}^{-2}$  but including also the spatial field envelope at positions in the focus corresponding to different gradients, and (c) at a peak intensity  $I_0 = 8.8 \text{ PW cm}^{-2}$  for the pure dipole approximation ( $D$ ) and additionally including the field envelope at  $w_0/2$  ( $D + G$ ) and full field (full). (d) As in (c), except for  $I_0 = 17.7 \text{ PW cm}^{-2}$ . (e) TDSE calculations for a 40 fs laser pulse ( $\cos^2$  envelope), in the dipole approximation at a peak intensity  $I_0 = 10 \text{ PW cm}^{-2}$  ( $D_1$ ); at an effective intensity  $I = 6 \text{ PW cm}^{-2}$  (which corresponds to  $u = w_0/2$ ) ( $D_2$ ); and as ( $D_2$ ), but with the field gradient ( $D_2 + G$ ).

field envelope effects due to the focusing of the laser beam strongly suppress excitation. Only at even higher intensities does the onset of field propagation, a genuine nondipole effect, fortify the suppression, but double ionization also sets in. Thus, the limit of the formation of the KH atom in optical laser fields as given by our investigation might be circumvented in a small intensity range by using a less focused laser beam, which then, however, requires higher laser pulse energy.

A. K., A. M., and A. S. acknowledge financial support from the German Federal Ministry of Education and Research within APPA R&D (Grant No. 05P15KHFAA).

\*zimmerma@mbi-berlin.de

†saenz@physik.hu-berlin.de

‡eichmann@mbi-berlin.de

- [1] M. Pont, N. R. Walet, M. Gavrilă, and C. W. McCurdy, Dichotomy of the Hydrogen Atom in Superintense, High-Frequency Laser Fields, *Phys. Rev. Lett.* **61**, 939 (1988).
- [2] M. V. Fedorov and A. M. Movsesian, Field-induced effects of narrowing of photoelectron spectra and stabilization of Rydberg atoms, *J. Phys. B* **21**, L155 (1988).
- [3] E. A. Volkova, A. M. Popov, and O. V. Smirnova, Stabilization of atoms in a strong field and the Kramers-Henneberger approximation, *Sov. Phys. JETP* **79**, 736 (1994).
- [4] W. C. Henneberger, Perturbation Method for Atoms in Intense Light Beams, *Phys. Rev. Lett.* **21**, 838 (1968).
- [5] M. Gavrilă, Atomic stabilization in superintense laser fields, *J. Phys. B* **35**, R147 (2002).
- [6] M. Pawlak and N. Moiseyev, Conditions for the applicability of the Kramers-Henneberger approximation for atoms in high-frequency strong laser fields, *Phys. Rev. A* **90**, 023401 (2014).
- [7] M. P. de Boer, J. H. Hoogenraad, R. B. Vrijen, L. D. Noordam, and H. G. Muller, Indications of High-Intensity Adiabatic Stabilization in Neon, *Phys. Rev. Lett.* **71**, 3263 (1993).
- [8] N. J. van Druten, R. C. Constantinescu, J. M. Schins, H. Nieuwenhuize, and H. G. Muller, Adiabatic stabilization: Observation of the surviving population, *Phys. Rev. A* **55**, 622 (1997).
- [9] M. Gavrilă, I. Simbotin, and M. Stroe, Low-frequency atomic stabilization and dichotomy in superintense laser fields from the high-intensity high-frequency Floquet theory, *Phys. Rev. A* **78**, 033404 (2008).
- [10] O. V. Smirnova, Validity of the Kramers-Henneberger approximation, *J. Exp. Theor. Phys.* **90**, 609 (2000).
- [11] Q. Wei, P. Wang, S. Kais, and D. Herschbach, Pursuit of the Kramers-Henneberger atom, *Chem. Phys. Lett.* **683**, 240 (2017).
- [12] F. Morales, M. Richter, S. Patchkovskii, and O. Smirnova, Imaging the Kramers-Henneberger atom, *Proc. Natl. Acad. Sci. U.S.A.* **108**, 16906 (2011).
- [13] U. Eichmann, T. Nubbemeyer, H. Rottke, and W. Sandner, Acceleration of neutral atoms in strong short-pulse laser fields, *Nature (London)* **461**, 1261 (2009).
- [14] M. Richter, S. Patchkovskii, F. Morales, O. Smirnova, and M. Ivanov, The role of the Kramers-Henneberger atom in the higher-order Kerr effect, *New J. Phys.* **15**, 083012 (2013).
- [15] P. B ejot, J. Kasparian, S. Henin, V. Loriot, T. Vieillard, E. Hertz, O. Faucher, B. Lavorel, and J.-P. Wolf, Higher-Order Kerr Terms Allow Ionization-Free Filamentation in Gases, *Phys. Rev. Lett.* **104**, 103903 (2010).
- [16] H. Zimmermann, S. Patchkovskii, M. Ivanov, and U. Eichmann, Unified Time and Frequency Picture of Ultrafast Atomic Excitation in Strong Laser Fields, *Phys. Rev. Lett.* **118**, 013003 (2017).
- [17] N. J. Kylstra, R. A. Worthington, A. Patel, P. L. Knight, J. R. V azquez de Aldana, and L. Roso, Breakdown of Stabilization of Atoms Interacting with Intense, High-Frequency Laser Pulses, *Phys. Rev. Lett.* **85**, 1835 (2000).
- [18] M. F orre and A. S. Simonsen, Nondipole ionization dynamics in atoms induced by intense xuv laser fields, *Phys. Rev. A* **90**, 053411 (2014).
- [19] E. Wells, I. Ben-Itzhak, and R. R. Jones, Ionization of Atoms by the Spatial Gradient of the Pondermotive Potential in a Focused Laser Beam, *Phys. Rev. Lett.* **93**, 023001 (2004).
- [20] S. Eilzer, H. Zimmermann, and U. Eichmann, Strong-Field Kapitza-Dirac Scattering of Neutral Atoms, *Phys. Rev. Lett.* **112**, 113001 (2014).
- [21] A. Ludwig, J. Maurer, B. W. Mayer, C. R. Phillips, L. Gallmann, and U. Keller, Breakdown of the Dipole Approximation in Strong-Field Ionization, *Phys. Rev. Lett.* **113**, 243001 (2014).
- [22] M. Klaiber and D. Dimitrovski, Survival of Rydberg atoms in intense laser fields and the role of nondipole effects, *Phys. Rev. A* **91**, 023401 (2015).
- [23] L. Ortmann, J. A. P erez-Hern andez, M. F. Ciappina, J. Sch otz, A. Chac on, G. Zeraouli, M. F. Kling, L. Roso, M. Lewenstein, and A. S. Landsman, Emergence of a Higher Energy Structure in Strong Field Ionization with Inhomogeneous Electric Fields, *Phys. Rev. Lett.* **119**, 053204 (2017).
- [24] T. Nubbemeyer, K. Gorling, A. Saenz, U. Eichmann, and W. Sandner, Strong-Field Tunneling without Ionization, *Phys. Rev. Lett.* **101**, 233001 (2008).
- [25] H. Zimmermann and U. Eichmann, Atomic excitation and acceleration in strong laser fields, *Phys. Scr.* **91**, 104002 (2016).
- [26] H. Zimmermann, J. Buller, S. Eilzer, and U. Eichmann, Strong-Field Excitation of Helium: Bound State Distribution and Spin Effects, *Phys. Rev. Lett.* **114**, 123003 (2015).
- [27] B. Quesnel and P. Mora, Theory and simulation of the interaction of ultraintense laser pulses with electrons in vacuum, *Phys. Rev. E* **58**, 3719 (1998).
- [28] M. V. Ammosov, N. B. Delone, and V. P. Krainov, Ionization in the field of a strong electromagnetic wave, *Sov. Phys. JETP* **64**, 1191 (1986).
- [29] N. B. Delone and V. P. Krainov, Energy and angular electron spectra for the tunnel ionization of atoms by strong low-frequency radiation, *J. Opt. Soc. Am. B* **8**, 1207 (1991).
- [30] See Supplemental Material at <http://link.aps.org/supplemental/10.1103/PhysRevLett.120.123202>, which includes Refs. [31–33], for details on the classical and quantum mechanical TDSE calculations.

- [31] X. M. Tong, Z. X. Zhao, and C. D. Lin, Theory of molecular tunneling ionization, *Phys. Rev. A* **66**, 033402 (2002).
- [32] U. Eichmann, A. Saenz, S. Eilzer, T. Nubbemeyer, and W. Sandner, Observing Rydberg Atoms to Survive Intense Laser Fields, *Phys. Rev. Lett.* **110**, 203002 (2013).
- [33] A. Lühr, Y. V. Vanne, and A. Saenz, Parameter-free one-center model potential for an effective one-electron description of molecular hydrogen, *Phys. Rev. A* **78**, 042510 (2008).
- [34] A. S. Simonsen and M. Førre, Magnetic-field-induced enhancement of atomic stabilization in intense high-frequency laser fields, *Phys. Rev. A* **92**, 013405 (2015).